

SIMULATION OF THE WORK OF A SPARK-IGNITION ENGINE WITH A DUAL-INJECTOR FUEL SYSTEM

Bronislaw Sendyka, Marcin Noga

*Cracow University of Technology
Institute of Automobiles and Internal Combustion Engines
Jana Pawła II Av. 37, 31-864 Krakow, Poland
tel.: +48 12 628 36 88, fax: +48 12 628 36 90
e-mail: bsendyka@pk.edu.pl, noga@pk.edu.pl*

Abstract

This paper is about computer modelling of a four-stroke spark-ignition engine with a dual-injector system. Using a KIVA-3V program for Linux, computer simulations were performed for one of the cylinders fuelled by multipoint injection and by the dual-injector system, i.e. with direct injection into the cylinders on top of MPI. The modelling was done for a combustion engine Toyota 2SZ-FE with a dual-injector system. Both simulations were done for the same parameters of engine's work, i.e. at the same RPM of 2000 and the intake pipe pressure of 0.079 MPa. KIVA-3V program models the processes taking place in an internal combustion engine while taking into account physical and chemical phenomena occurring during the formation of a charge and during its combustion. Using a stochastic model of injection the program takes into account the movement of droplets and their dispersion. The results of the simulation show that the dual-injector system has an improved volumetric coefficient, i.e. improved engine performance. An increase in the engine's indicated pressure was also observed; this increases the engine's total efficiency. The intensification of the charge's angular momentum in a cylinder with a dual-injector system can explain the improvements in the course of combustion process. Because the air-fuel mixture was already partially formed in the engine there was a small increase in the unburned hydrocarbons in the cylinder. However, a marked drop in the carbon monoxide and nitric oxide were observed for the dual-injector system. Analyzing the overall results of the simulations one can ascertain a positive impact of using a dual-injector system on the working parameters of a spark-ignition engine.

Keywords: *dual-injector fuel system, direct injection, port injection, combustion, spark-ignition engine, modelling, simulation, KIVA-3V*

1. Introduction

To describe the effects of using a dual-injector system in a tested engine, its work was simulated in a KIVA-3V program run on a 64 bit Linux system. The engine under consideration was a four-stroke spark-ignition engine from Toyota Yaris. An important structural change is the installation on the cylinder head the injectors necessary to inject fuel directly to the cylinders. In this way the dual-injector system was built. It allows for the injection of fuel to the intake port as well as directly into the combustion chamber. The idea behind this fuel system was described in more detail in [8, 9], while [6] contains a more detailed account of a test rig set-up. The placement of the injectors in relation to the combustion chamber is presented in Fig. 1.

2. Modelling injection, formation of the charge and combustion

KIVA-3V program models in 3D the processes that take place inside the cylinder. It accounts for the physical and chemical phenomena occurring during the formation of the charge and during its combustion [1-3, 5].

The program accounts for the movement of droplets and their dispersion. Using a stochastic model of injection it is assumed that the injector forms a conical stream of fuel of a certain length and width. A model of stream formation and its dispersion is shown diagrammatically in Fig. 2.

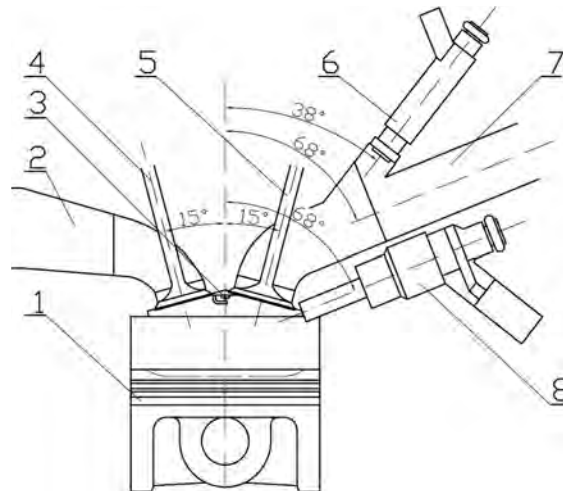


Fig. 1. Placement of the injectors for direct injection to the cylinder and to intake port 1 - Piston 2 - Exhaust port, 3 - spark plug electrodes, 4 - Exhaust valve, 5 - Intake valve, 6 - MPI injector, 7 - Intake port, 8 - Direct injector

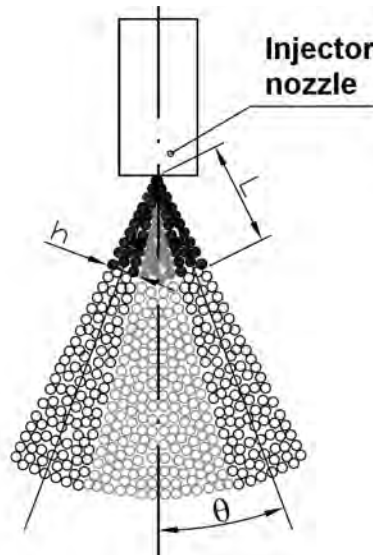


Fig. 2. Diagrammatical representation of formation and dispersion of a fuel stream coming out of the injector's nozzle

Undispersed droplets were marked with solid colour. Black colour denotes droplets visible in the longitudinal cross-section of the stream. The basic parameters describing the fuel stream leaving the nozzle are: length L , width h and top angle 2θ . Distance L from the jet's nozzle is the distance at which the process of dispersion of the droplets starts and it is calculated using the Clark-Dombrowski equation [5]:

$$L = B \cdot \left(\frac{\rho_{pal} \cdot \sigma \cdot \ln(\eta / \eta_p) \cdot h \cdot \cos \theta}{\rho_{ot}^2 \cdot v^2} \right)^{1/2}, \quad (1)$$

where:

B - constant ($B=3$ [5]),

ρ_{pal} - fuel density, kg/m^3 ,

σ - fuel's surface tension, N/m ,

h - width of the fuel stream, m ,

ρ_{ot} - density of surrounding gas, kg/m^3 ,

v - relative speed between gas and fuel stream, m/s ,

η - amplitude of the pressure wave in the moment of droplet dispersion, m ,

η_p - amplitude of the pressure wave before droplet dispersion, m .

The width h of the stream coming from the injector's nozzle can be derived from equation (2).

$$h = \left(A \cdot \frac{12 \cdot \mu_{pal} \cdot \dot{m}_{pal} \cdot (1+X)}{\pi \cdot d_0 \cdot \rho_{pal} \cdot \Delta p_{inj} \cdot (1-X)^2} \right)^{\frac{1}{2}}, \quad (2)$$

where:

- h - width of the stream coming from the injector's nozzle, m,
- A - constant, from the geometry of the injector, average value assumed to be 400 [5],
- μ_{pal} - kinematical viscosity of fuel coefficient, Pa·s,
- \dot{m}_{pal} - intensity of fuel flow, kg/s,
- Δp_{inj} - difference in pressures between the fuel and the combustion chamber, Pa,
- X - constant that depends on technical parameters of the injector used, -,
- ρ_{pal} - fuel density, kg/m³.

The velocity of the injected fuel stream is described by formula (3) and it comes directly from Bernoulli's equation and the continuity equation.

$$v_{inj} = C_d \cdot \sqrt{\frac{2 \cdot \Delta p_{inj}}{\rho_{pal}}}, \quad (3)$$

where:

- v_{inj} - velocity of the injected fuel stream, m/s,
- C_d - injector flow coefficient, -,
- Δp_{inj} - difference in pressures between the fuel and the combustion chamber, Pa,
- ρ_{pal} - fuel density, kg/m³.

Angle θ depends on the design of the injector's nozzle. For the direct injection nozzles it usually takes on a value between 30 and 37°.

Next, we consider the dispersion of the fuel droplets as a result of the forces working on them as described by the following differential equation (4).

$$\frac{d^2 y_{dr}}{dt^2} + \frac{5 \cdot \mu_{pal}}{\rho_{pal} \cdot r_{dr}^2} \frac{dy_{dr}}{dt} + \frac{8 \cdot \sigma}{\rho_{pal} \cdot r_{dr}^3} y_{dr} - \frac{2}{3} \cdot \frac{\rho_{pal} \cdot v^2}{\rho_{ot} \cdot r_{dr}^2} = 0, \quad (4)$$

where:

- r_{dr} - radius of the fuel droplet before dispersion, m,
- y_{dr} - deformation of the droplet (in relation to droplet's radius), -,
- t - time, s.

The rest of variables as above.

The dispersion of the droplet is only possible when $y_{dr} > 1$ [5]. In such a case the size of the droplets is determined based on the balance of energy before and after the droplet's dispersion and is described by equation (5).

$$\frac{r_{dr1}}{r_{dr2}} = \frac{7}{3} + \frac{1}{8} \frac{\rho_{pal} \cdot r_{dr1}^3}{\sigma} \left(\frac{dy_{dr1}}{dt} \right)^2, \quad (5)$$

where:

- 1,2 - indices denoting the state of droplets before and after it is dispersed.

The rest of variables as above.

In the next step, the KIVA-3V program takes into account the evaporation of the fuel droplets as described by the Spalding's model [7]; the low pressure evaporation where its speed is described by the following equation (6).

$$\frac{dm_{dr}}{dt} = -2\pi \cdot r_{dr} \cdot \rho_{ot} \cdot D \cdot B_M \cdot Sh, \quad (6)$$

where:

m_{dr} - droplet's mass, kg,

D - diffusion of the mass of fuel vapours into gas, m^2/s ,

B_M - Spalding's coefficient for the flow of mass from droplets into gas, -,

Sh - Sherwood's coefficient of the mass flow, -.

The rest of variables as above.

KIVA-3V allows for simulation of the engine's work using different types of fuel. In this paper a hydrocarbon fuel with a chemical formula of C_8H_{17} was used. One can see a similarity to octane (C_8H_{18}), but it approximates more closely the real petrol's mass proportions between carbon and hydrogen in a particle. This is the reason it can be treated as a special kind of one-ingredient petrol. C_8H_{17} fuel is oxidized according to the following reaction (7):



Fuel combustion described by the chemical equation (7) is the main chemical reaction taking place during the simulation in the KVA-3V program. Other important for the outcome chemical processes take place according to equations (8), (9), and (10).



The set of reactions (8) through (10) describes the so called thermal mechanism of the formation of the nitric oxide, which takes place in high temperatures, like those occurring during the combustion process in the cylinders. It is called an expanded Zeldovich mechanism, after the Russian researcher Jakov Zeldovich who described it.

The simulation work was concentrated on finding out and comparing the differences between the processes of combustion taking place in a cylinder fuelled by multipoint injection and for that fuelled by dual-injection.

To make this simulation work possible, a spatial grid of one of the cylinders of our engine had to be prepared and the modifications to the KIVA-3V program be made to allow for the simulation of both injectors simultaneously, a feature not present in the program's basic configuration.

3. The simulation of the engine's operation

The engine model used in this research was prepared on the available technical data on the Toyota 2SZ-FE engine. The parameters needed to prepare a spatial grid such as the geometric data of the cylinder head and the characteristics of the valve lift were obtained by physically measuring the elements of the our modified engine. For simulation purposes the crankshaft position was set to open at piston position 4° CA before TDC (top dead centre), and the closing ending at 46° CA after BDC (bottom dead centre). This reflects the work of the test engine during research trials with the variable valve timing system deactivated.

The computational grid prepared with the aid of the KIVA-3V program has 35 horizontal layers, with more layers at the top to obtain more accurate results. Fig. 3 represents a cross section along the valve axis for the piston position 156° CA after TDC, i.e. in the period of intake stroke.

On the above picture the top of the combustion chamber is clearly outlined as well as the partially open intake valve.

A general view of the spatial grid from the side of the intake port at piston position 66° CA after TDC is presented in Fig. 4.

In KIVA-3V part of the simulation parameters is set independently for the so-called regions. First region is the cylinder's working volume, second is the intake pipe and the third the exhaust port. The layout of the regions in the engine under consideration is presented in a diagram in Fig. 5.

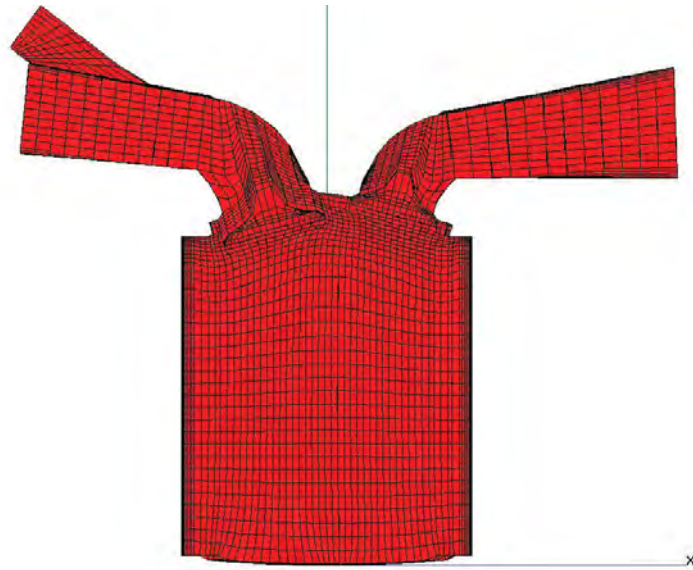


Fig. 3. A cross section along the valve axis for the piston position 156 ° CA after TDC

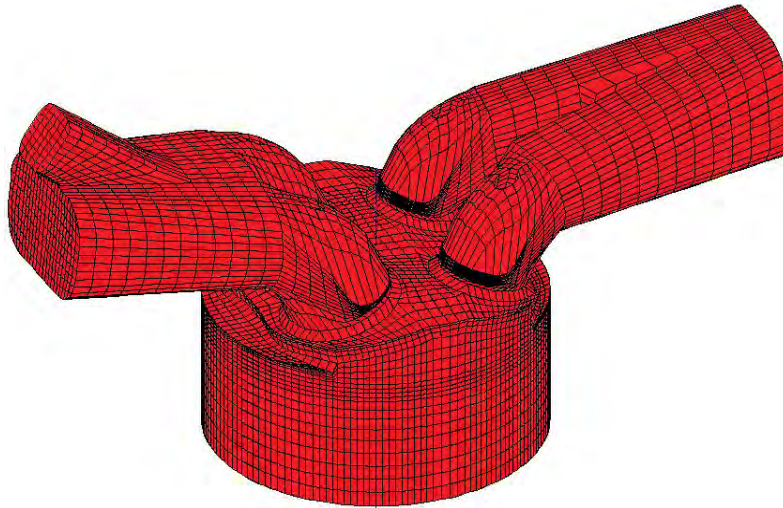


Fig. 4. A general view of the grid from the side of the intake port at piston position 66° CA after TDC

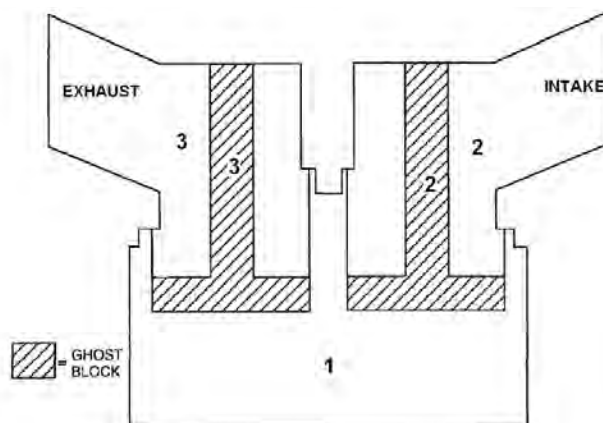


Fig. 5. Layout of the regions in the engine under consideration [2]; 1 - Cylinder's working volume, 2 - Intake port, 3 - Exhaust port

The valves are described as a „ghost block”, i.e. outside elements which have the ability to move in relation to the mesh.

4. Initial conditions

For both simulations (for multipoint injection and dual-injection) the stoichiometric composition of the mixture stayed the same. In both cases the absolute pressure in the intake port was assumed to be 0.079 MPa, and the same position of the throttle as during the tests on the test stand.

A dose of fuel to intake port was 0.01610 g for one work cycle (for multipoint injection system). For the simulation of the dual-injector system this was divided between the multipoint and direct injection with the direct injection's fraction of the total at 0.63. The meant that 0.0060 g of fuel was injected into the intake port and 0.0101 g of fuel was injected directly into the combustion chamber. The total dose in this case was 0.01661 g/cycle, which is slightly more than for multipoint injection.

The beginning of the injection to the intake port for both simulation was at TDC, i.e. right after the intake valves were open, while the beginning of the injection to the combustion chamber was set at piston position 79° CA after TDC. Both simulations were performed for the crankshaft speed of 2000 RPM and the advanced angle of ignition of 14° CA. The total time of the spark discharge (all phases: spark-over, electric arc, glow) was taken to be 1.33 ms, which for the given RPM is around 16° CA. A pressure in the exhaust port was assumed to be 0.11 MPa. The outside pressure was assumed at 0.097 MPa.

In the simulations done the temperatures of the various elements of the engine were averaged out and set as constants. The temperature of the cylinder sleeve was 450 K, cylinder head wall 500K, and the piston head 530 K. This simplification does not have a significant effect on the accuracy of the results while significantly cutting down the time of the calculations.

During the simulations 12 different chemical substances were considered. It should also be mentioned at this point that the KIVA-3V program uses the turbulence model of k- ϵ type (k – kinetic energy of the turbulence, ϵ – dissipation of this energy) [1].

5. A comparison of the results for the two injection systems

Fig. 6. represents a comparison of pressures in the cylinder's working volume as a function of the crankshaft angle for both types of systems: multipoint injection (MPI) and the combined injection (DI+MPI). There is a visible difference of the maximum pressure and the slightly bigger surface area under the curve of the dual-injector system (DI+MPI).

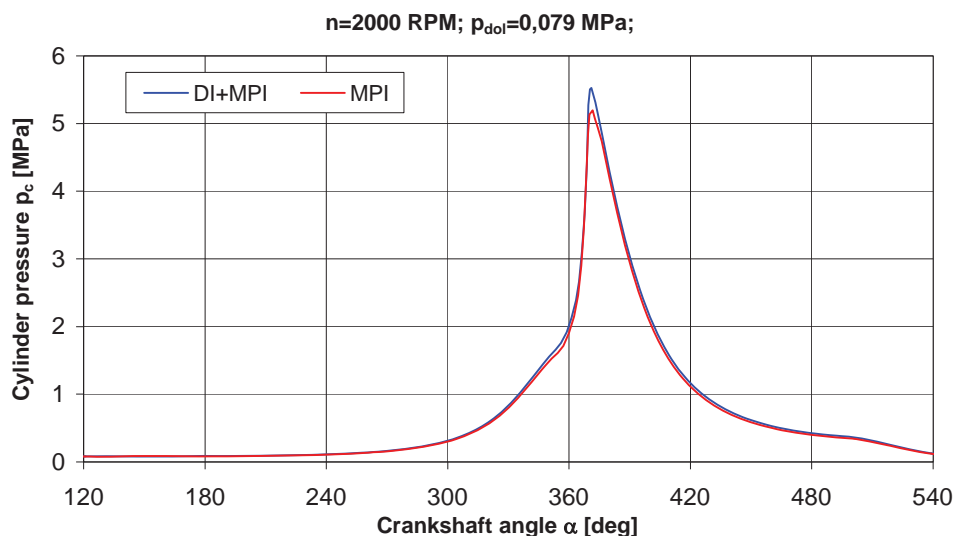


Fig. 6. Comparison of pressures p_c in the cylinder's volume as a function of the crankshaft angle α for both types of systems

Figure 7 contains the closed indicated diagrams based on the information from Fig. 6.

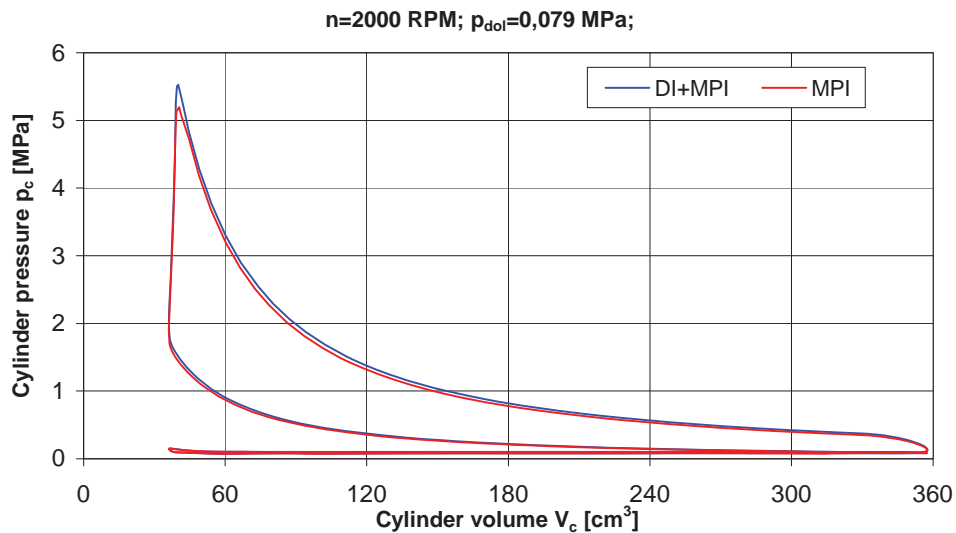


Fig. 7. Pressure changes in the cylinder p_c as a function of the cylinder volume V_c obtained in the simulations of both systems

To better illustrate the differences in pressures for the two systems from Fig. 7, an enlarged parts of the closed indicating diagrams are shown in Fig. 8.

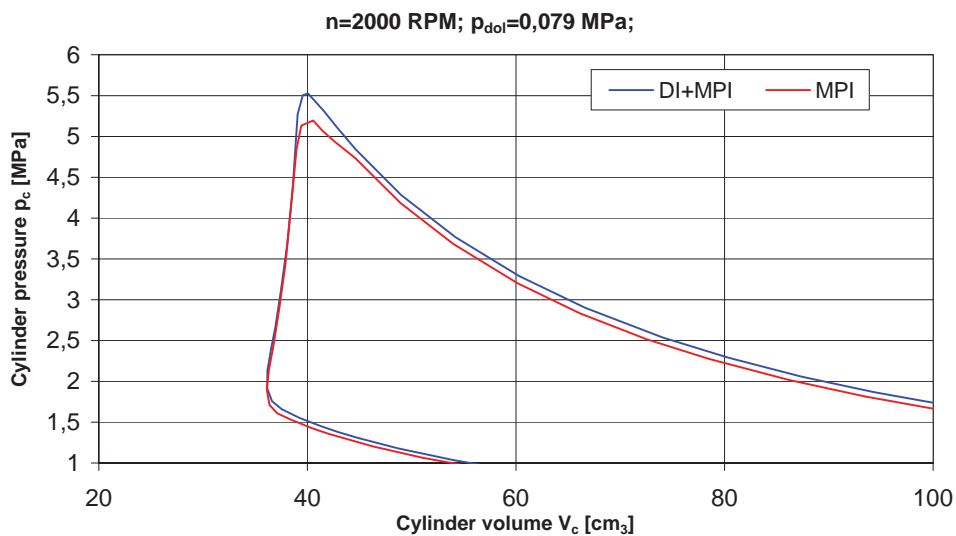


Fig. 8. Enlarged portion of the closed indicator diagram illustration the difference in the process of supplying heat for both injection systems

Changes in temperature of the charge for the two systems are illustrated in Fig. 9.

The visible differences between the curves in Fig. 9 derived from the simulation of the two types of injection systems are similar to the ones for the changes in pressure in the cylinder's working volume.

Fig. 10 shows the change in the mass of fuel for both systems as a function crankshaft angle.

In the case of the multipoint injection, during the time period under consideration, in the cylinder there are only the fuel vapours. When dual-injection is used, the part of fuel injected directly into the cylinder evaporates completely even before the moment of ignition. This is represented on a diagram when the green curve reaches the level of zero (the mass of the liquid

fuel) and the maximum level by the blue curve (mass of the vaporized fuel), which takes place at around 120° CA before TDC, while the advanced ignition angle in the simulation was 14° CA.

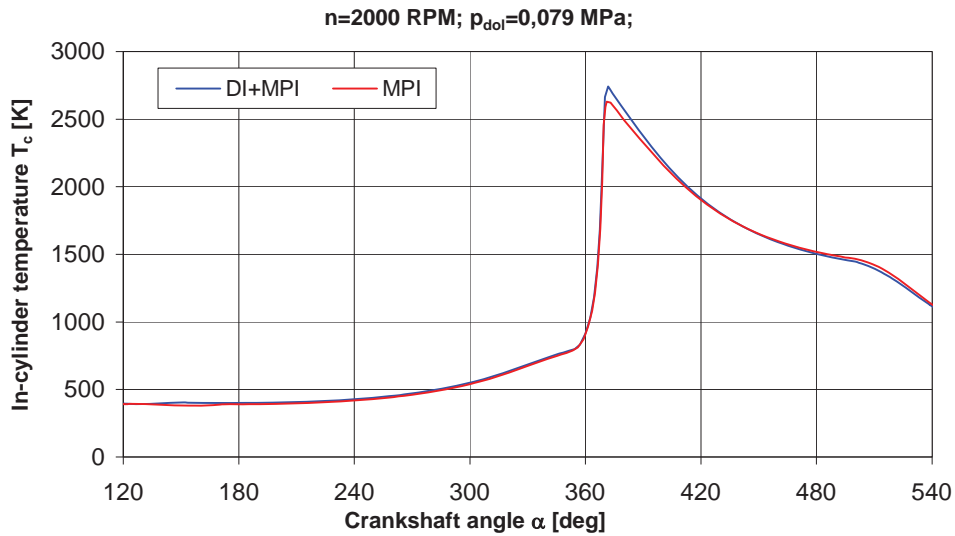


Fig. 9. Changes in temperature in the cylinder for the dual-injector system and the multipoint injection

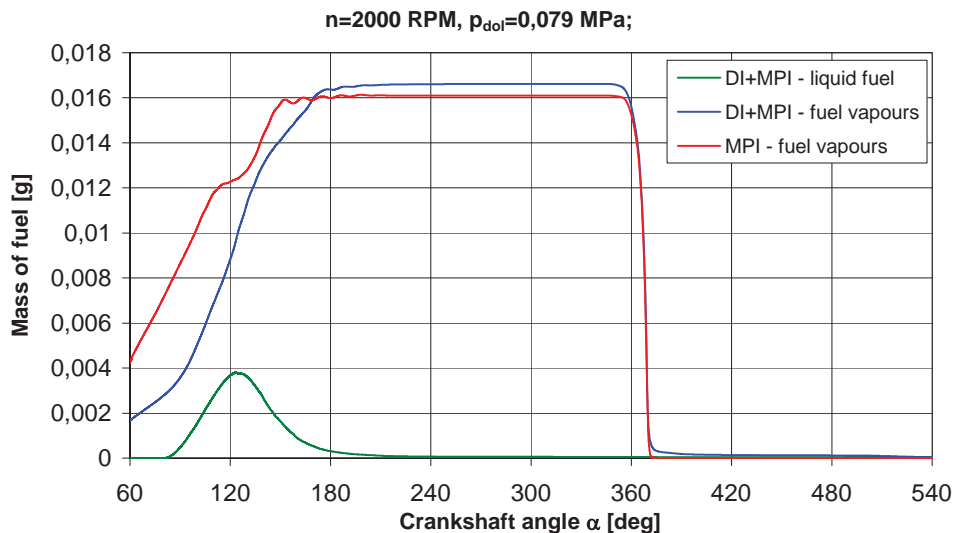


Fig. 10. Change in the mass of fuel in the cylinder for the two injection system

Angular momentum of the charge is the combined measure of the swirl and tumble movements which affect the intensity of the fuel evaporation, its dispersion in the cylinder's working volume, and, in effect, the velocity of the flame propagation. The KIVA program calculates the angular momentum of the charge in relation to three axes of coordinates. The graphs of the changes of in the angular momentum of the charge in the cylinder against the three axes of coordinates for multipoint injection system are shown in Fig. 11.

Changes in the angular momentum of the charge K as a function of the crankshaft angle for dual-injection system are shown in Fig. 12.

There is a significant impact on the dose of fuel injected directly into the cylinder. In the case of combined injection, angular momentum K reaches higher values during the intake and compression stages than for the MPI. The increased angular momentum against the "y" axis can be interpreted as the intensification of the tumble, while the increased angular momentum against the vertical axis of the cylinder "z" can be interpreted as the intensification of the swirl [4].

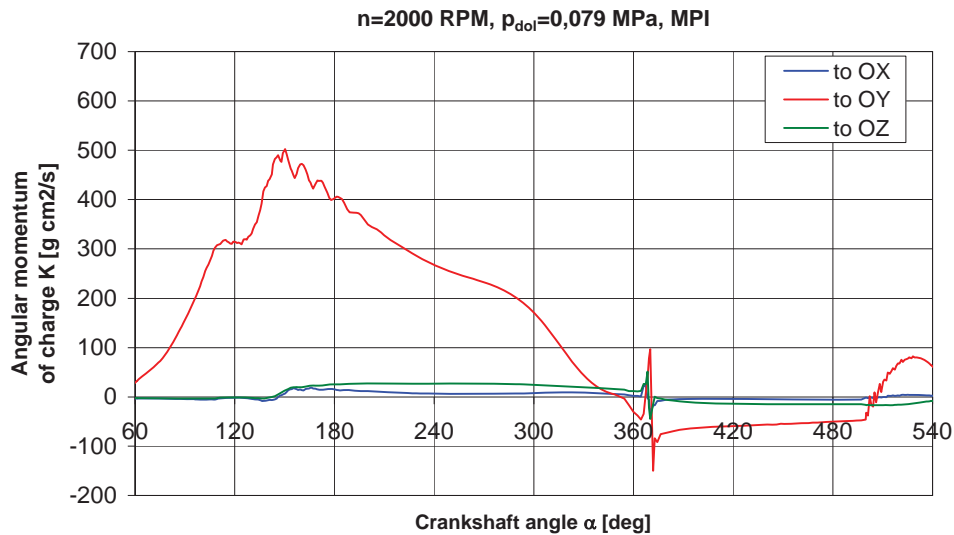


Fig. 11. Angular momentum of charge K against the three axes as a function of the crankshaft angle α for MPI

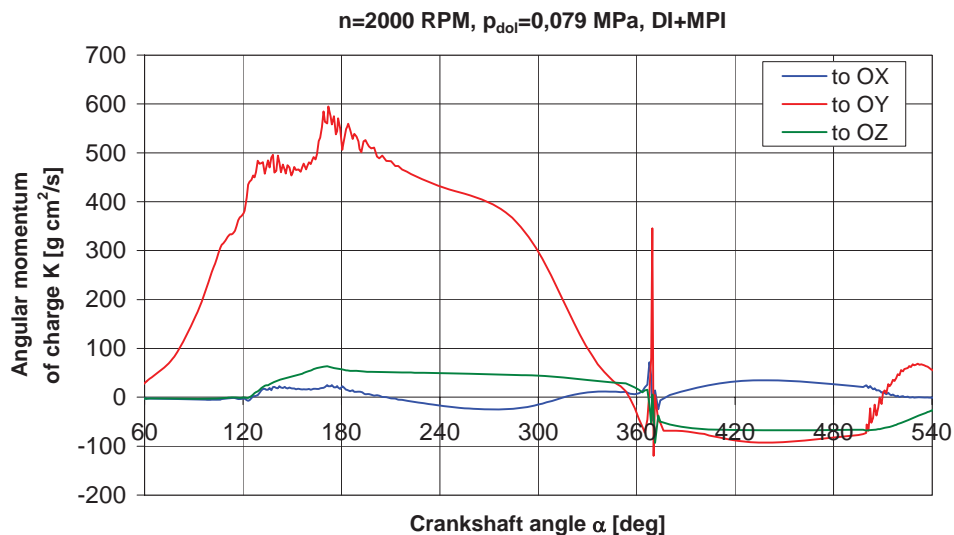


Fig. 12. Angular momentum of charge K against the three axes as a function of the crankshaft angle α for dual-injection system

Based on Fig. 11 and Fig. 12 the changes in angular momentum against single axes of coordinates, as a function of the crankshaft angle are shown in Fig. 13.

The intensified turbulence of the charge in the cylinder shown in Fig. 11-13 has a significant effect of improving the combustion process and because of that it increases the torque generated by the engine. On the following diagrams you can see the fraction of mass of the hydrocarbons HC, carbon monoxide CO and nitric oxide NO in the cylinder, as a function of the crankshaft angle. Fig. 14 for the MPI and Fig. 15 for the combined injection.

The analysis of the graphs in Fig. 14 and Fig. 15 shows that there are differences in concentrations of carbon monoxide CO, hydrocarbons HC and nitric oxide NO between the two injection systems. After the combustion process is finished in the combustion chamber there is a bigger concentration of CO and NO for the MPI when compared to the dual-injection system. The dual-injection, however, has a higher concentration of unburned hydrocarbons. The difference is about 80ppm, which is not a significant amount.

Fig. 16 shows the fraction of the fuel mass in the cross section of the cylinder's working volume during the intake stroke for MPI.

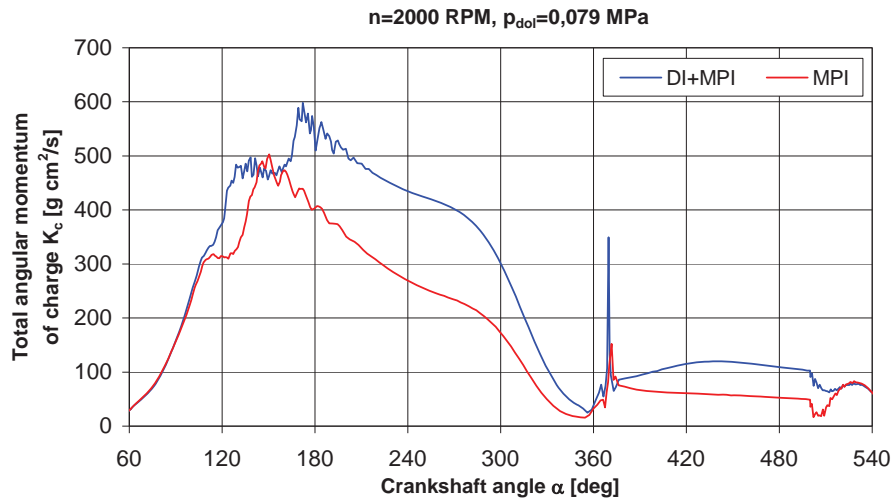


Fig. 13. Total angular momentum K_c against single axes of coordinates, as a function of the crankshaft angle for both injection systems

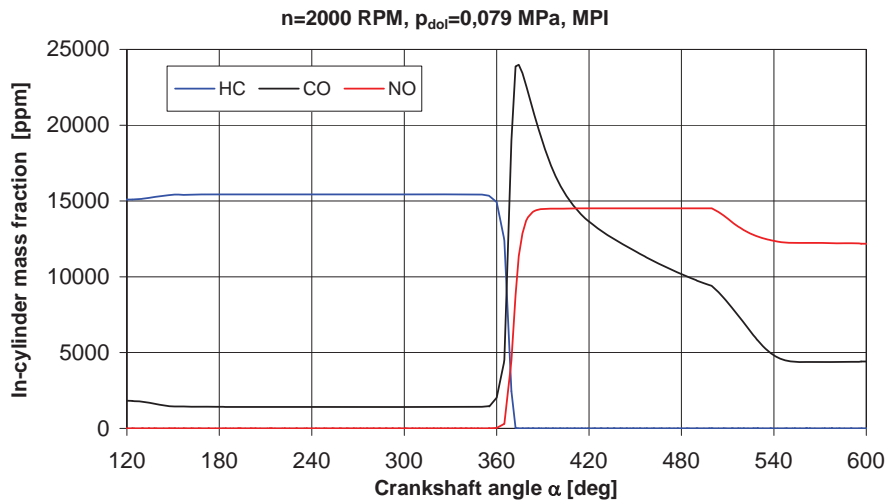


Fig. 14. Fraction of mass of the hydrocarbons HC, carbon mono oxide CO and nitric oxide NO in the cylinder as a function of the crankshaft angle for MPI

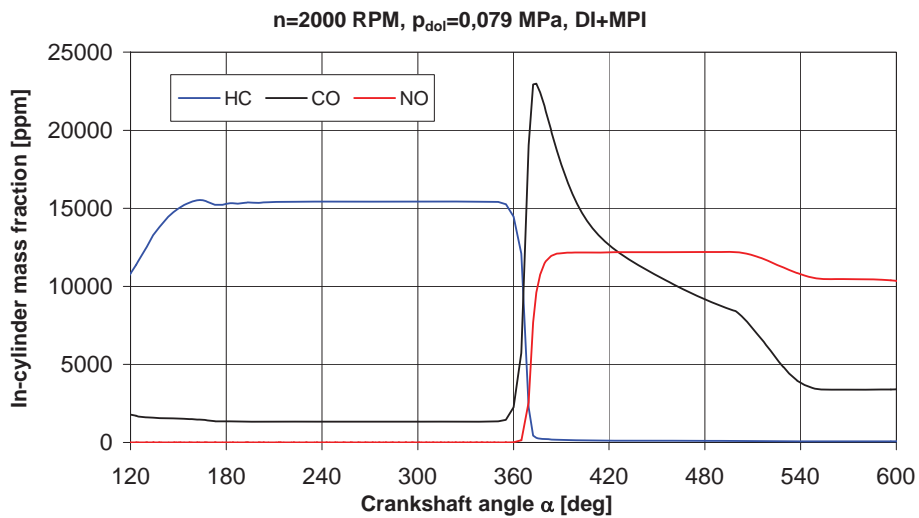


Fig. 15. Fractions of mass of HC, CO and NO in the cylinder as a function of the crankshaft angle for the dual-injection

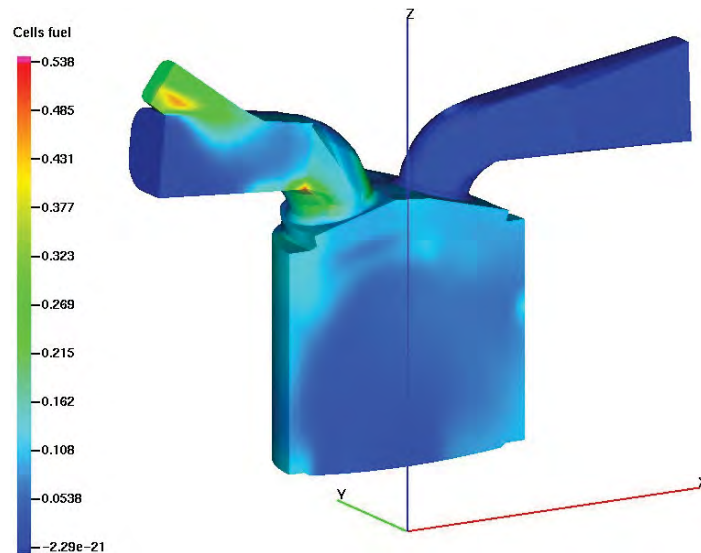


Fig. 16. Fraction of fuel mass in the cylinder of MPI, piston position – 250° CA before TDC

The same visualisation for the dual-injection is displayed in Fig. 17.

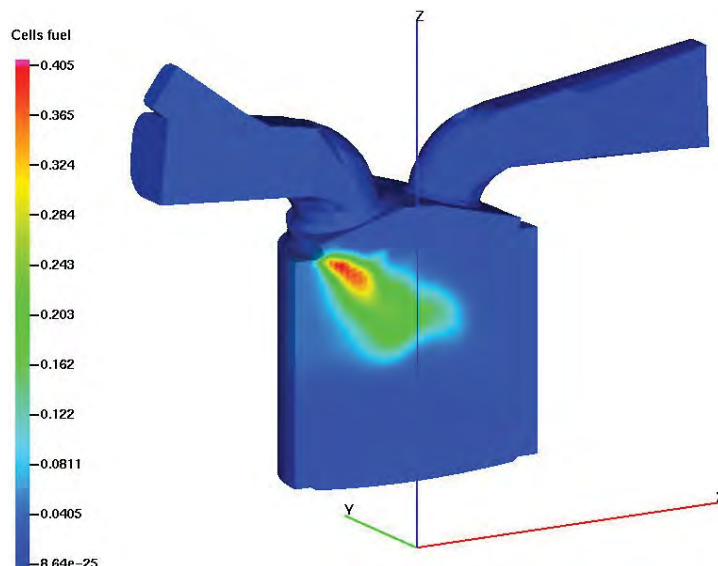


Fig. 17. Fraction of fuel mass in the cylinder for dual-injection, piston position – 250° CA before TDC

In Fig. 17 one can clearly see the stream of fuel injected directly into the cylinder.

6. Conclusions

The simulations of the engine working with MPI or a dual-injection system allow for the following conclusions:

- To obtain the same value of the air excess coefficient for the dual-injection as for the MPI requires a slightly bigger dose of fuel. This points to an improved volumetric efficiency for the dual-injection for the conditions set in the simulation.
- The injection of fuel directly into the cylinder during the intake stroke causes an intensification of the charge's turbulence. The measure of this process is an increase in the total angular momentum during the intake stroke. This is a beneficial phenomenon which has a positive effect on the formation of the combustible mixture and, in effect, on the combustion process which occurs later.

- It was observed that for dual-injection the whole mass of the charge evaporates more than 100° CA before ignition. The time required to form a homogenous mixture is relatively long.
- For the dual-injection the maximum combustion pressure is about 6% higher when compared to the MPI. The average rate of pressure rise $dp_c/d\alpha$ from the moment of ignition to when the maximum combustion pressure is reached is 0.16 MPa/°CA, slightly higher than it is for the MPI (0.15 MPa/°CA).
- The working cycle of the engine with dual-injection is characterized by a 3% higher mean indicated pressure than the engine with MPI.

In conclusion, the simulation work performed here shows that it is well worth to perform engine trials with a dual-injection system.

References

- [1] Amsden, A., *KIVA-3: A KIVA Program with Block-Structured Mesh for Complex Geometries*, LA-1 2503-MS, UC-361, Los Alamos National Laboratory, Los Alamos 1993.
- [2] Amsden, A., *KIVA-3V, Release 2, Improvements to KIVA-3V*, LA-13608-MS, Los Alamos National Laboratory, Los Alamos 1999.
- [3] Amsden, A., O'Rourke, P. J., Butler, T. D., *KIVA-II, A computer program for chemically reactive flows with sprays*, Los Alamos National Laboratory LA-11560-MS, Los Alamos 1989.
- [4] Kowalewicz, A., *Wybrane zagadnienia samochodowych silników spalinowych*, Wydanie 2, poprawione i uzupełnione, Wydawnictwo Politechniki Radomskiej, Radom 2002.
- [5] Mitianiec, W., *Wtrysk paliwa w silnikach dwusuwowych małej mocy*, Wydawnictwo Instytutu Gospodarki Surowcami Mineralnymi i Energią. Polska Akademia Nauk, Kraków 1999.
- [6] Sendyka, B., Noga, M., *Determination of optimal fuel mass relation dosed by a dual-injector fuel system in a spark ignition engine*, Silniki Spalinowe 2009-SC2, PTNSS–2009–SC–123, PTNSS, Bielsko-Biała 2009.
- [7] Spalding, D. B., *The Combustion of Liquid Fuels*, 4th Symposium of Combustion, William & Wilkins, 1953.
- [8] Tsuji, N., Sugiyama, M., Abe, S., *Der neue 3.5L V6 Benzinmotor mit dem innovativen stöchiometrischen Direkteinspritzsystem D-4S*, 27. Internationales Wiener Motorensymposium, Austria 2006.
- [9] Yamaguchi, J. K., *Lexus gives V6 dual injection. 2006 Engine Special Report*, Automotive Engineering International January 2006, pp. 17 – 20, SAE International, Warrendale 2006.